



ELSEVIER

Nuclear Instruments and Methods in Physics Research B 178 (2001) 62–68

NIM B
Beam Interactions
with Materials & Atoms

www.elsevier.nl/locate/nimb

Colloidal assemblies modified by ion irradiation

E. Snoeks^a, A. van Blaaderen^{a,b}, T. van Dillen^a, C.M. van Kats^b, K. Velikov^b,
M.L. Brongersma^a, A. Polman^{a,*}

^a FOM Institute for Atomic and Molecular Physics, Kruislaan 407, 1098 SJ, Amsterdam, The Netherlands

^b Debye Institute, Utrecht University, P.O. Box 80.000, 3508 TA, Utrecht, The Netherlands

Abstract

Spherical SiO₂ and ZnS colloidal particles show a dramatic anisotropic plastic deformation under 4 MeV Xe ion irradiation, that changes their shape into oblate ellipsoidal, with an aspect ratio that can be precisely controlled by the ion fluence. The 290 nm and 1.1 μm diameter colloids were deposited on a Si substrate and irradiated at 90 K, using fluences in the range 3×10^{13} – 8×10^{14} cm⁻². The transverse particle diameter shows a linear increase with ion fluence, while the longitudinal diameter shrinks; the particle volume remains constant. Size aspect ratios up to 3.1 are achieved. Applications of the ion beam deformation technique are shown in studies of liquid crystalline colloidal ordering, self-assembled two-dimensional colloidal lithographic masks for thin-film deposition, and in tuning the optical properties of three-dimensional colloidal crystals. © 2001 Elsevier Science B.V. All rights reserved.

Keywords: Colloid; Ion irradiation; Anisotropic deformation; Liquid crystal; Nanolithography; Colloidal crystal

1. Introduction

One of the many [1] effects that ion irradiation can have on a material is anisotropic deformation. This effect, that was first observed for free-standing thin films composed of a metallic glass irradiated at energies of several 100 MeV [2,3], causes the irradiated region to expand in the direction perpendicular to the ion beam, and to shrink in the direction of the beam. More recently, anisotropic plastic strain generation has also been observed in thin films that are constrained to a substrate, using

irradiation at 4 MeV [4,5]. In the latter case, it leads to the build-up of a steady-state mechanical stress in the irradiated region, of which the magnitude is determined by the balance between the expansion rate and radiation-induced Newtonian viscous flow [6] that serves to relax stress. So far, anisotropic deformation has been found to occur in amorphous materials only. It is thought to be the result of the high electronic energy deposition ($> \text{keV/nm}$) and low directional straggle in the ion trajectory that cause a cylindrically shaped narrow thermal spike to evolve around the ion track [7,8]. Plastic relaxation of the local shear stress induced by thermal expansion of this hot cylindrical region can result in plastic deformation perpendicular to the cylindrical axis.

* Corresponding author. Tel.: +31-20-608-1234; fax: +31-20-668-4106.

E-mail address: polman@amolf.nl (A. Polman).

In this paper, we study the effect of anisotropic growth on colloidal particles. This enables to study the deformation effect in three independent orientations with respect to the ion beam. In addition, as we will show, it leads to a shape change of the colloids from spherical to ellipsoidal, that can be controlled with great accuracy. Colloidal particles play an important role in studies of self-assembly and phase behavior, and can find many applications in practical materials with interesting optical properties. A system of optically transparent ellipsoidal colloids with adjustable aspect ratio would be ideal to investigate the effect of anisotropic particle shape on phase behaviour or optical properties [9–11]. By exploiting the ion beam deformation technique these studies now become possible, as we will show.

2. Experimental

Two dispersions of colloidal silica (SiO_2) spheres in ethanol, with diameters of 290 and 1030 nm were synthesized through hydrolysis and condensation reactions from tetra-ethoxysilane as described in [12]. Drops of a dilute dispersion were placed on the clean surface of a Si(001) substrate, after which the ethanol solvent was left to evaporate. Some experiments were performed on ZnS colloids, fabricated using a method similar to that described in [13,14]. These particles were spherical with a diameter of 1170 nm and consist of aggregates of cubic sphalerite nanocrystals [15]. ZnS/silica core-shell particles (ZnS core diameter 168 nm, total diameter 255 nm), made as described in [15], were also irradiated.

The deposited particles were irradiated with 4 MeV Xe^{4+} ions with the sample surface held at an angle of $+45^\circ$ with respect to the direction of the ion beam, as indicated in the schematic inset in Fig. 1. The ion beam was electrostatically scanned to homogeneously irradiate the entire sample. The beam flux was in the range $(3\text{--}8) \times 10^{10}$ ions/ cm^2s and the ion fluences ranged from $3 \times 10^{13}\text{--}8 \times 10^{14}$ cm^{-2} . The Si substrate was tightly clamped against a copper sample stage that was cooled to 90 K using liquid nitrogen. The base pressure during ion irradiation was 5×10^{-7} mbar.

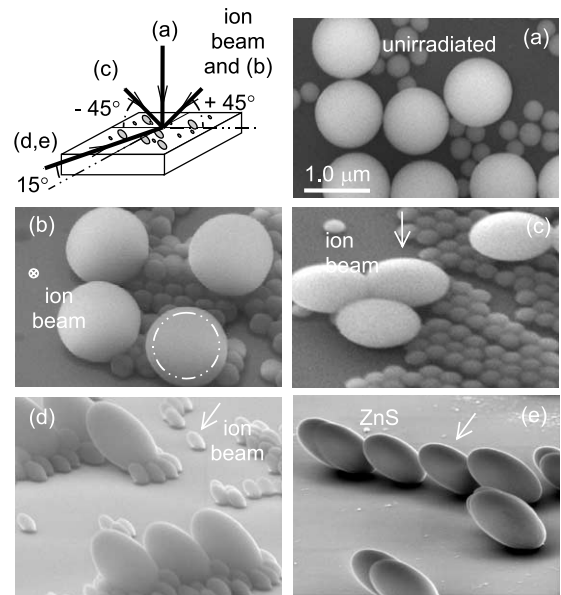


Fig. 1. SEM images of silica (a)–(d) and ZnS (e) particles on a Si substrate: (a) top view (0° tilt) of as-deposited silica spheres with two different diameters; (b)–(d) silica spheroids after 4 MeV Xe irradiation to a fluence of 3×10^{14} cm^{-2} , under an angle of $+45^\circ$, at 90 K. The ion beam direction and the different viewing angles are indicated in the schematic inset for each image; (e) ZnS microspheres irradiated with 5×10^{14} Xe/cm^2 under an angle of 45° at 90 K. All images are taken at the same magnification.

The projected mean ion range of 4 MeV Xe ions into colloidal silica is around $1.9 \mu\text{m}$.¹

In studies where the irradiated particles were removed from the substrate, a carbon-coated glass slide was used as a substrate, and was covered for only 1% with 1030-diameter silica spheres, to avoid interaction between deforming particles. By ultrasonic treatment the irradiated particles did easily detach from the surface while the carbon layer did not detach, most probably as a result of cohesion enhancement due to ion beam mixing.

Before and after irradiation, particle shapes were analysed using a Philips XL30 FEG scanning electron microscope (SEM) operating at 10 kV. Optical transmission measurements on colloidal crystals were made under normal incidence, using a Varian Cary 500 spectrophotometer employing a

¹ Assuming a density of $2.00 \text{ g}/\text{cm}^3$.

white light source, a grating spectrometer, and photomultiplier and Ge photodetectors.

3. Results

3.1. Anisotropic deformation of silica colloids

Fig. 1(a) shows a SEM image of the silica spheres on the Si surface, viewed under normal incidence to the substrate before irradiation. The two different particle sizes are easily distinguished, and the diameters are sharply centred around 290 and 1030 nm, with a relative size polydispersity $\sigma = 3\%$. Figs. 1(b), (c) and (d) show SEM images taken after irradiation to a fluence of 3×10^{14} ions/cm². The images were obtained using different sample tilt angles in the microscope. The three (almost) orthogonal projections provide a full identification of the particle shape after irradiation: expansion is observed in the plane normal to the direction of the ion beam, and contraction in the direction of the beam. In Fig. 1(b) these spheroids are viewed along the direction of the ion beam, i.e., at a $+45^\circ$ tilt angle as indi-

cated in the schematic inset. In this particular projection, the spheroids appear circular. The dashed circle represents the circumference of unirradiated spheres. The projected diameters of both the large and small particles have increased by 24%. The two images taken perpendicular to the ion beam, Figs. 1(c) and (d), show the elliptically shaped side views of the spheroids. The cross-sectional size of the deformed particles along the direction of the ion beam decreased with respect to the original diameter by about 35%.

Experiments as described above were performed for various Xe ion fluences ranging from 3×10^{13} to 8×10^{14} ions/cm². Fig. 2 shows the average transverse and longitudinal diameter of the spheroids as obtained from SEM micrographs as a function of fluence, for the large (a) and small (b) particles. The deformation increases monotonically with fluence and the aspect ratio of the most strongly deformed spheres in Fig. 2 is 3.11 ± 0.13 . The drawn line corresponds to a linear increase in the transverse particle diameter with fluence, while the dashed curve shows how the longitudinal axis must shrink if the volume of the spheroids would remain constant. Both curves describe the data quite well, indicating that the volume of the particles does not significantly change during the deformation process. The curves shown in Figs. 2(a) and (b) for the large and small particles are identical, apart from a size scaling factor. This implies that surface tension does not affect the particle deformation. We have performed deformation experiments using different ion fluxes in the range $(3-8) \times 10^{10}$ cm⁻² s⁻¹, and found that the total deformation for a given total ion fluence is independent of the ion flux used.

The particles shown so far have all been obtained using 4 MeV Xe⁴⁺ ion irradiation at 90 K. We have also studied beam-induced deformation of silica spheres at room temperature. We found that the particles deform in the same way as at 90 K, but at a rate that is about a factor four slower. This agrees well with measurements of the temperature dependence of the deformation rate derived from mechanical stress measurements on planar silica films irradiated with 4 MeV Xe [1].

The observed macroscopic deformation is the result of the integrated effect of a large number of

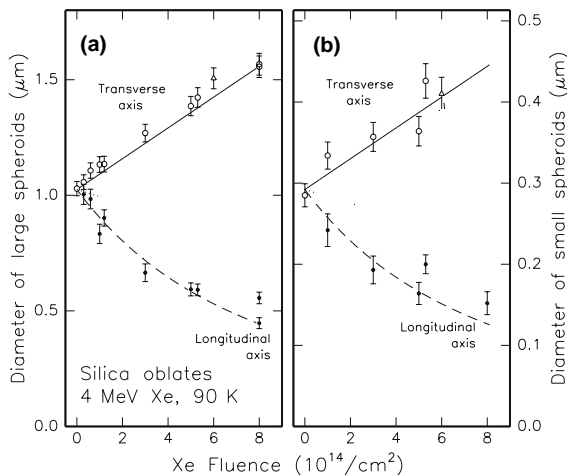


Fig. 2. Transverse and longitudinal diameters of large (a) and small (b) silica spheres as a function of 4 MeV Xe⁴⁺ irradiation fluence. All irradiations were performed at 90 K. The line drawn through the data for the transverse axis is a linear fit, the dashed line is a calculation derived from the drawn line assuming the particle volume remains constant with fluence.

microscopic single ion impacts. Note that at a fluence of 8×10^{14} ions/cm² each 1030 nm diameter particle has been impacted by some 10^7 Xe ions. Over such large numbers any statistical variations are expected to average out, so that the deformed particles are expected to be very monodisperse in both size and shape. Indeed, measurements of the size polydispersity before and after irradiation, reported in [16], show that relative standard deviation in the size distribution ($\sigma = 3\%$) for the large silica colloids remains unaltered after irradiation.

To prove that the deformation is indeed the result of the anisotropic nature of the thermal spike around the 4 MeV ion track, experiments were also performed using 500 keV Xe⁴⁺ ions.² The energy loss rate at this energy is roughly equal to that for 4 MeV, but in this case atomic collisions rather than electronic energy loss dominate the energy deposition. This leads to a much higher lateral ion straggle and hence a less anisotropically shaped excited region. Indeed, no plastic deformation of silica colloids was observed after irradiation at an energy of 500 keV, even to a fluence as high as 1×10^{16} cm⁻².

It is interesting to note that, while a linear increase in the transverse diameter of the spheroids is observed in Fig. 2, an exponential growth of the transverse lengths with fluence would be expected if the deformation rate (per ion) would be constant with fluence. This implies that the deformation rate decreases with ion fluence. To account for the behaviour observed in Fig. 2 we have to assume that the deformation strain per ion gradually decreases from 6.6 to 4.3×10^{-16} cm²/ion for the fluence range studied. This change with fluence may be due to a structural or compositional change of the silica during ion irradiation [17].

We have also performed experiments in which deformed colloids were irradiated a second time under a direction orthogonal to the first irradiation (direction (c) in the inset of Fig. 1) [18]. In this way prolate (sugar-shaped) ellipsoids were made, proving the beam-directional anisotropy of the defor-

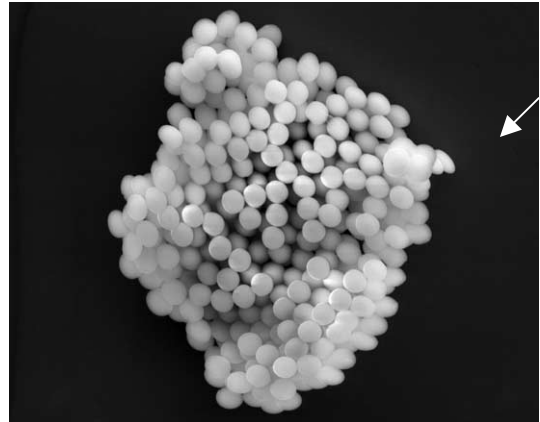


Fig. 3. SEM image of silica spheroids obtained by 4 MeV Xe⁴⁺ irradiation of 1030 nm diameter spheres. After irradiation the particles were brought in ethanol suspension by ultrasonic treatment. This solution was then slowly dried on a silicon substrate. The arrow indicates a spheroid along the edge of the cluster that shows no ordering but gives an impression of the size aspect ratio.

mation effect. By using repeated irradiations from different directions much more complex shaped particles than ellipsoids may be made as well.

3.2. Anisotropic deformation of other materials

We have also investigated the anisotropic deformation of colloidal ZnS spheres. Fig. 1(e) shows a SEM image of these ZnS particles after 4 MeV Xe⁴⁺ irradiation. As can be seen, these ZnS microspheres are deformed into spheroids as well; the size aspect ratio equals 2.2 ± 0.2 . As these ZnS particles have a relatively high refractive index, several optical applications of these deformed particles can be envisioned, as will be discussed in Section 3.5.

As noted before, anisotropic deformation has so far only been observed on amorphous materials, while the present ZnS colloids are microcrystalline. More research is required to study if the colloids have amorphized during irradiation. We have also found that amorphous TiO₂ colloids show strong deformation, while polycrystalline Al₂O₃ and Ag colloids do not show deformation under 4 MeV Xe irradiation to a fluence of 4×10^{14} cm⁻² at 90 K.

² Here only the smaller particles (with 290 nm diameter) were used because the ion range of 500 keV Xe in silica is about 280 nm (see note 1).

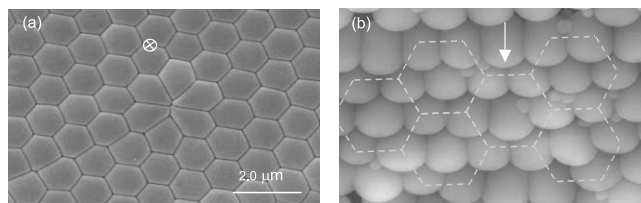


Fig. 4. SEM images of a hexagonally close-packed monolayer of 1030 nm diameter silica particles after irradiation: (a) after irradiation under normal incidence using 4 MeV Xe^{4+} ions to a fluence of $7.5 \times 10^{14} \text{ cm}^{-2}$. The remnants of a dislocation in the original structure, terminated by a vacancy, are clearly seen; (b) after irradiation under 45° off the surface normal (at an azimuth indicated by the arrow) to a fluence of $3 \times 10^{14} \text{ Xe/cm}^2$. The dashed lines indicate the original hexagonal arrangement. Both (a) and (b) are imaged normal to the surface, and both irradiations are performed at 90 K.

3.3. Anisotropic colloidal liquid crystals

Preliminary investigations were performed of the phase behaviour of suspensions of ellipsoidal colloids. To this end, silica spheroids with an aspect ratio of 2.75 ± 0.11 were brought back into ethanol suspension by ultrasonic treatment. A stable suspension of deformed silica particles in solution was obtained and light scattering confirmed that the spheroids were redispersed as single entities. Fig. 3 shows a SEM image of a structure formed by these spheroids after they were concentrated by slowly drying the dispersion on the surface of a Si substrate. The figure clearly shows that the particles have dried into a nematic-like structure with clear directional order (with the director pointing out of the plane of the image) and no positional order. Close to the edge of the structure some of the spheroids have a different orientation (see e.g. the arrow in Fig. 3). This arrangement does not only show that (the majority of) the spheroids have indeed been suspended as individual particles, but also gives strong indications that concentrated dispersions of these spheroids will form a nematic colloidal liquid crystalline phase. Computer simulations predict that oblate ellipsoids with an aspect ratio of 2.75 and higher can form such a nematic phase [9,10]. Nematic-isotropic phase transitions in dispersions of hard plate-like colloids have been observed only recently for a system of gibbsite platelets [19]. However, because of their relatively high size and shape polydispersity and hexagonal shape, comparison of the phase behaviour of such particles with computer simulations is much more difficult

than for the ellipsoidal particles made using the ion irradiation technique.

3.4. Anisotropic deformation of two-dimensional colloidal crystals, nanolithography

Next, we show the effect of MeV ion irradiation on colloidal spheroids that are assembled in a two-dimensional ordered structure. A hexagonally close-packed structure of 1030 nm diameter silica spheroids on a silicon substrate was irradiated with 4 MeV Xe^{4+} ions under normal incidence to a fluence of $7.5 \times 10^{14} \text{ cm}^{-2}$ at 90 K. Fig. 4(a) shows a SEM image after irradiation. As can be seen, the particles that were originally spherical have deformed quite strongly and fill completely the empty space between particles. Even a vacancy, that was present in the original unirradiated structure and that terminated a dislocation coming in from the lower left, is completely filled up as a result of the deformation. The structure in Fig. 4(a) is completely different to what would be observed if the colloids had been deformed by purely thermal treatment [20].

Fig. 4(b) shows a hexagonally packed monolayer of silica particles irradiated under an angle of 45° at a fluence of $3 \times 10^{14} \text{ Xe/cm}^2$. As can be seen in the SEM image, taken normal to the surface, this results in an interesting structure of partially overlapping rows of particles, reminiscent of shingles or roof tiles. The anisotropy is caused by the fact that due to the sample tilt during irradiation the particles were free to expand in one direction perpendicular to the ion beam, but constrained in the other direction due to the

presence of neighboring particles. Such anisotropic colloidal films are expected to show highly anisotropic optical properties.

The deformation of regular colloidal structures can also be used to tailor the shape of microspheroids comprising a self-assembled lithographic mask for thin-film deposition [21,22]. In this way the lattice spacing and shape of the voids in between the spheres can be uncoupled. As a preliminary example of this effect we show in Fig. 5 SEM images of a Au pattern formed after electron-beam deposition through a close-packed hexagonal arrangement of 1030 nm diameter silica colloids placed on a Cr-coated glass substrate (a), and after evaporation through a similar colloidal layer that was first irradiated under normal incidence with 4 MeV Xe at 90 K at a fluence of $3 \times 10^{14} \text{ cm}^{-2}$ (b). After deposition the colloidal mask was removed. In the SEM images the Cr substrate appears dark, while the deposited Au appears light grey. Although these data only give a qualitative demonstration of the effect, a reduction in feature size of the Au dots using the deformed colloidal mask (Fig. 5(b)) is clearly seen.

3.5. Anisotropic deformation of three-dimensional colloidal crystals

Finally, we show how the optical properties of a three-dimensional photonic colloidal crystal can be modified using ion irradiation. In these experiments, core-shell particles consisting of a 168 nm diameter ZnS core covered by a 44 nm thick silica

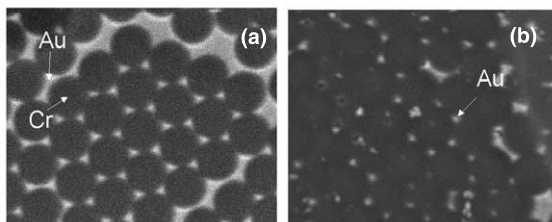


Fig. 5. Au patterns on a Cr-coated glass substrate made by deposition through a self-assembled colloidal mask that was (a) unirradiated, or (b) deformed with 4 MeV Xe ions at 90 K to a fluence of $3 \times 10^{14} \text{ cm}^{-2}$ under normal incidence. The images were taken under normal incidence, after removal of the colloids. In the images Cr appears dark, and Au appears light grey.

shell were assembled in a three-dimensional hexagonally close-packed crystal structure consisting of five layers in the direction perpendicular to the substrate, as determined using SEM. The crystal was irradiated using 4 MeV Xe to a total ion fluence of $4 \times 10^{14} \text{ cm}^{-2}$ at an incident angle of 45° at 90 K. The ion range is well beyond the crystal thickness.

Fig. 6 shows the optical transmission spectrum of the colloidal crystal, measured under normal incidence, before and after irradiation. The spectrum before irradiation shows clear oscillations, that are attributed to interference due to Bragg scattering between the crystal planes. The overall decrease for small wavelengths is due to the increased scattering off the colloidal particles. After irradiation, the transmission yield for large wavelengths remains unaltered, indicating that the ion irradiation itself does not cause absorption in the colloids. However, a large difference is observed in the low wavelength interference structure. For example, the Bragg minimum that occurs at a wavelength of 616 nm before irradiation shifts to 575 nm after irradiation. This shift is ascribed to the combined effect of changes in the crystal

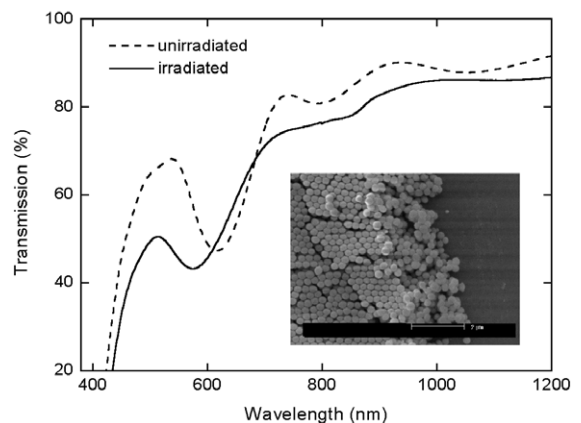


Fig. 6. Optical transmission spectra for a three-dimensional photonic crystal composed of five layers of 255-nm diameter ZnS/silica core-shell particles, ordered in a hexagonally close-packed structure. Data are shown before and after irradiation with 4 MeV Xe⁴⁺ ions to a fluence of $4.0 \times 10^{14} \text{ cm}^{-2}$ under an angle of 45° at 90 K. A shift in the Bragg minimum from 616 to 575 nm is clearly seen. The inset shows a SEM image of the edge of the crystal taken before irradiation.

symmetry and particle form factor due to the ion irradiation, and possibly a small crystal contraction. These measurements clearly demonstrate that the optical properties of three-dimensional photonic structures can be modified in a controllable way using ion irradiation. When combined with methods that allow control over the orientation and symmetry of two- and three-dimensional colloidal crystals [23,24] the particle deformation technique will also provide for an important additional degree of freedom to tune optical phenomena in (thin) photonic crystals. In fact, optical bandstructure calculations show that, for a given particle asymmetry, photonic crystals composed of spheroids can have larger bandgaps than those composed of spheres [25]. Also, it has been shown that a single oblate micro-resonator shows strongly improved lasing properties compared to a spherical resonator [11].

4. Conclusions

MeV ion irradiation of colloidal silica and ZnS particles leads to a dramatic anisotropic deformation, in which the particles plastically expand in the direction perpendicular to the ion beam, and shrink in the direction along the ion beam. The transverse axis of the ellipsoidal oblate particles shows a linear increase with ion fluence, and a size aspect ratio as large as 3.1 is achieved. After irradiation the particles can be resuspended in solution and a preliminary demonstration of nematic liquid crystalline ordering of ion-beam deformed ellipsoids is presented. The effect of ion beam induced deformation on two-dimensional colloidal crystals is also shown and a preliminary application in self-assembled colloidal lithographic masks is presented. Finally, it is shown that anisotropic deformation can modify the optical properties of a three-dimensional colloidal crystal.

Acknowledgements

We gratefully acknowledge J.H.M. Dos Santos for some of the initial ion irradiations. This work is part of the research program of the Foundation

for Fundamental Research on Matter (FOM), which is financially supported by the Dutch Foundation for Scientific Research (NWO).

References

- [1] M.L. Brongersma, E. Snoeks, T. van Dillen, A. Polman, *J. Appl. Phys.* 88 (2000) 59.
- [2] M.-D. Hou, S. Klaumünzer, G. Schumacher, *Phys. Rev. B* 41 (1990) 1144.
- [3] A. Benyagoub, S. Löffler, M. Rammensee, S. Klaumünzer, G. Seamann-Ischenko, *Nucl. Instr. and Meth. B* 65 (1992) 228.
- [4] E. Snoeks, A. Polman, C.A. Volkert, *Appl. Phys. Lett.* 65 (1994) 2487.
- [5] E. Snoeks, T. Weber, A. Cacciato, A. Polman, *J. Appl. Phys.* 78 (1995) 4723.
- [6] M.L. Brongersma, E. Snoeks, A. Polman, *Appl. Phys. Lett.* 71 (1997) 1628.
- [7] H. Trinkaus, A.L. Ryazanov, *Phys. Rev. Lett.* 74 (1995) 5072.
- [8] M.L. Brongersma, E. Snoeks, A. Polman, *Appl. Phys. Lett.* 71 (1997) 1628.
- [9] D. Frenkel, B.M. Mulder, *Mol. Phys.* 55 (1985) 1171.
- [10] J.A. Veerman, D. Frenkel, *Phys. Rev. A* 45 (1992) 5632.
- [11] J.U. Noeckel, A.D. Stone, *Nature* 385 (1997) 45.
- [12] A. van Blaaderen, A. Vrij, *Langmuir* 8 (1993) 2921 (and references cited).
- [13] S.M. Scholz, R. Vacassy, J. Dutta, H. Hofmann, M. Akinc, *J. Appl. Phys.* 83 (1998) 7860.
- [14] S.M. Scholz, R. Vacassy, L. Lemaire, J. Dutta, H. Hofmann, *Appl. Organometal. Chem.* 12 (1998) 327.
- [15] A.K.P. Velikov, A. van Blaaderen, To be published. (Preliminary results were published in: A. van Blaaderen, *MRS Bulletin* 23 (1998) 39).
- [16] T. van Dillen, A. van Blaaderen, A. Polman, W. Fukarek, *Appl. Phys. Lett.* 78 (2001) 910.
- [17] N. Moriya, Y. Shacham-Diamand, R. Kalish, *Appl. Phys. Lett.* 57 (1990) 108.
- [18] E. Snoeks, A. van Blaaderen, T. van Dillen, C.M. van Kats, M.L. Brongersma, A. Polman, *Adv. Mater.* 12 (2000) 1511.
- [19] F.M. van der Kooij, H.N.W. Lekkerkerker, *J. Phys. Chem. B* 102 (1998) 7829.
- [20] H. Míguez, F. Meseguer, C. Lopez, A. Blanco, J.S. Moya, J. Requena, A. Mifsud, V. Fornes, *Adv. Mater.* 10 (1998) 480.
- [21] N.D. Denkov, O.D. Velev, P.A. Kralchevsky, I.B. Ivanov, H. Yoshimura, K. Nagayama, *Langmuir* 8 (1992) 3183.
- [22] F. Burmeister, C. Schäfle, T. Matthes, M. Böhmisch, J. Boneberg, P. Leiderer, *Langmuir* 13 (1997) 2983.
- [23] A. van Blaaderen, R. Ruel, P. Wiltzius, *Nature* 385 (1997) 321.
- [24] A. van Blaaderen, *MRS Bulletin* 23 (1998) 39.
- [25] J.W. Haus, H.S. Sözüer, R.J. Inguva, *J. Mod. Opt.* 39 (1992) 1991.